



Power Electronic Systems
Laboratory

© 2011 IEEE

Proceedings of the 8th International Conference on Power Electronics (ECCE Asia 2011), The Shilla Jeju, Korea,
May 30-June 3, 2011.

„Magnetic Ear“ - Based Balancing of Magnetic Flux in High Power Medium Frequency Dual Active Bridge Converter Transformer Cores

G. Ortiz
J. Mühlethaler
J.W. Kolar

This material is posted here with permission of the IEEE. Such permission of the IEEE does not in any way imply IEEE endorsement of any of ETH Zurich's products or services. Internal or personal use of this material is permitted. However, permission to reprint/republish this material for advertising or promotional purposes or for creating new collective works for resale or redistribution must be obtained from the IEEE by writing to pubs-permissions@ieee.org. By choosing to view this document, you agree to all provisions of the copyright laws protecting it.



Eidgenössische Technische Hochschule Zürich
Swiss Federal Institute of Technology Zurich

"Magnetic Ear"-Based Balancing of Magnetic Flux in High Power Medium Frequency Dual Active Bridge Converter Transformer Cores

G. Ortiz, J. Mühlethaler, and J. W. Kolar
 Power Electronic Systems Laboratory, ETH Zurich
 ETL I16, Physikstrasse 3
 CH-8092 Zurich, Switzerland
 Email: ortiz@lem.ee.ethz.ch

Abstract—Semiconductor switches possess non-ideal behavior which, in case of isolated DC-DC converters, can generate DC voltage components in the voltage applied to the transformer. This DC voltage component is translated into a DC flux density component in the transformer core, increasing the risk of driving the core into saturation. In this paper, a novel non-invasive flux density measurement principle, called the "Magnetic Ear", based on sharing of magnetic path between the main and an auxiliary core is proposed. The active compensation of the transformer DC magnetization level using this transducer is experimentally verified. Additionally, a classification of the previously reported magnetic flux measurement and balancing concepts is performed.

I. INTRODUCTION

Isolated and/or high step-up DC-DC converters are built with arrangements of semiconductor switches which provide AC excitation to a transformer. Phenomena such as unmatched turn-on/turn-off times, semiconductor forward voltage drop, gate driving signal delays or pulsating load, among others, can cause differences in the positive and negative volts-seconds applied to the transformer [1]. This results in a DC voltage component at the transformer terminals, which causes an undesired DC magnetic flux density component in the transformer core.

To show the relation between this voltage and magnetic flux density DC components, consider the circuit presented in Fig. 1-a), where a Dual Active Bridge (DAB) DC-DC converter topology is shown. The primary and secondary bridges apply voltages $v_p(t)$ and $v_s(t)$ to the transformer respectively. The DC and the AC components of these voltages can be separated into independent voltage sources, building the circuit depicted in Fig. 1-b), where the secondary side has been reflected to the primary side. Here, the resistances $R_{p,T}$ and $R'_{s,T}$ represent the winding resistances $R_{p,s}$ and $R'_{s,s}$ plus the semiconductors' equivalent on-state resistances of the primary and secondary side switches respectively.

In steady state, the DC magnetizing current $I_{m,DC}$ of the transformer is given by

$$I_{m,DC} = I_{p,DC} - I'_{s,DC} = \frac{V_{p,DC}}{R_{p,T}} - \frac{V'_{s,DC}}{R'_{s,T}} \quad (1)$$

The DC magnetic flux density is then determined by the characteristics of the winding and core through

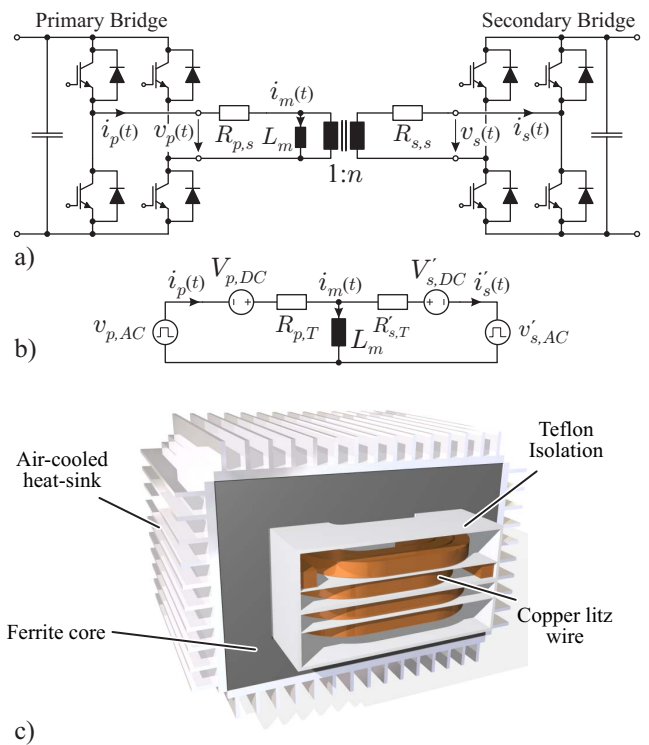


Fig. 1. a) DAB converter with simplified transformer model; b) Equivalent model of the converter with independent DC and AC voltage sources and reflected secondary side; c) Shell-type transformer optimized for efficiency

$$B_{DC} = \frac{I_{m,DC} \cdot N_p}{l_m} \cdot \mu_0 \bar{\mu}_r = \left(\frac{V_{p,DC}}{R_{p,T}} - \frac{V'_{s,DC}}{R'_{s,T}} \right) \cdot \frac{N_p}{l_m} \cdot \mu_0 \bar{\mu}_r \quad (2)$$

where l_m is the length of the magnetic path, N_p is the number of turns in the primary side, μ_0 is the permeability of air and $\bar{\mu}_r$ is the core's relative permeability in the linear region of the B-H curve.

From (2) it can be seen that the DC magnetic flux density is limited by the equivalent series resistances, $R_{p,T}$ and $R'_{s,T}$,

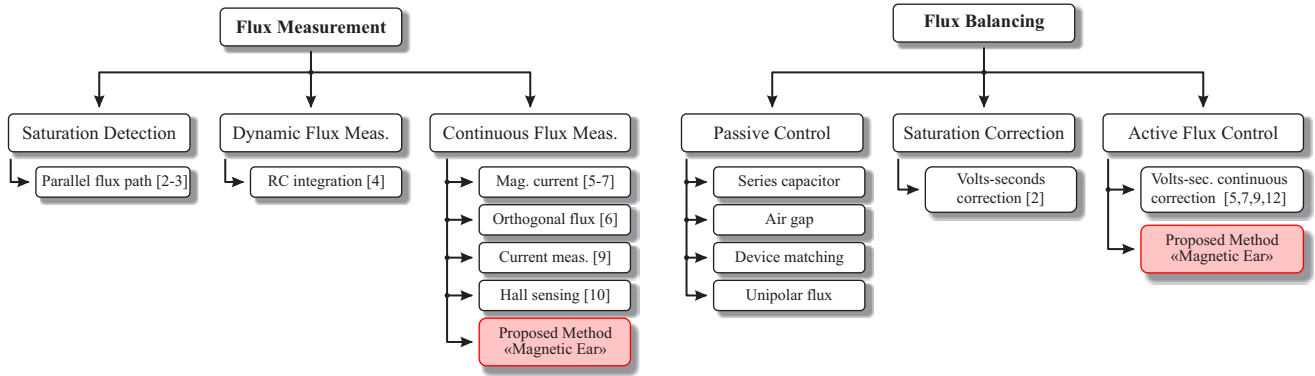


Fig. 2. Classification of previously proposed flux balancing concepts. The two main areas are flux measurement and flux feedback control. The proposed measurement concept, the "Magnetic Ear", is highlighted within this classification.

of the circuit, which are typically kept as low as possible in order to decrease the converter's conduction losses. This means that a small DC component in the voltage applied to the transformer generates a large DC flux density component.

For example, taking the shell-type 166 kW/20 kHz efficiency-optimized transformer (cf. Fig. 1-c) with suitable switches on the primary side, the primary side equivalent resistance $R_{p,T}$ reaches 1.7 m Ω . This design considers a Ferrite N87 core material which is characterized by a relative permeability $\bar{\mu}_r$ around 1950. In this design, a 0.00125% of relative difference in the duration of the positive and negative semicycles of the primary voltage $v_s(t)$, i.e. a switching time error of 0.25 ns, would suffice to create a DC flux density component of $B_{DC} = 50$ mT.

With this DC flux density component, the core can be easily driven outside the linear region of the B-H curve, generating a non-linear magnetizing current with high peak values. This results in increased conduction and switching losses, causing reduction in efficiency and higher semiconductor and transformer operating temperatures which could ultimately destroy the converter. Moreover, a DC biased flux density waveform results in higher core losses, further compromising the converter's efficiency. For these reasons, the operation of the transformer under balanced conditions, i.e. with zero DC flux density component, must be ensured. It is also worth to note that if a balanced operation of the flux density in the core is ensured, the transformer can be designed with low flux density over-dimensioning, meaning that its magnetic cross section, and therefore its volume, can be reduced, increasing the converter's power density.

In this paper, a novel magnetic flux density transducer is introduced and its operating principle is experimentally verified. The measured transducer signal is used to perform a closed-loop flux balancing control, ensuring the operation of the transformer core within safe flux density values. First, in **Section II**, a classification of previously proposed methods which enable detection of saturation and/or continuous measurement of the flux density behavior is laid out along with methods to balance the transformer's internal flux density. The proposed flux density transducer is described in **Section III** together with experimental testing. In **Section IV** the output signal of the transducer is used to perform a closed-loop compensation of the flux density in the transformer core.

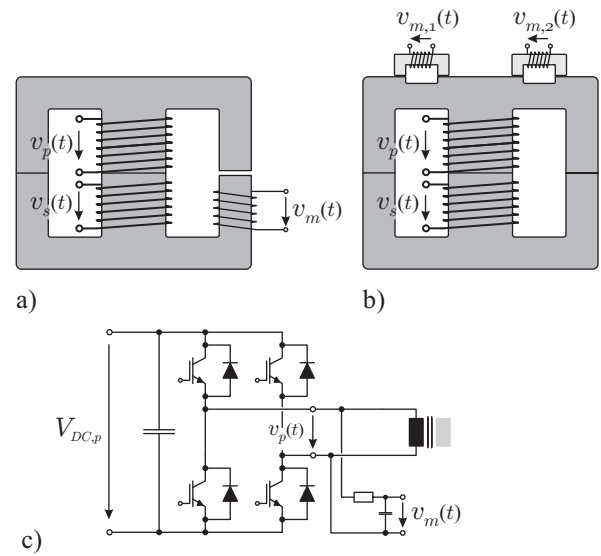


Fig. 3. Previously proposed concepts for magnetic saturation prevention: a) Parallel magnetic path in an E-core with an gaped leg [2]; b) Parallel magnetic path with external cores and reduced cross section [3]. c) Integration of applied voltage with RC network [4].

II. CLASSIFICATION OF FLUX MEASUREMENT/CONTROL METHODS

In order to ensure balanced flux operation, the main problems that must be addressed are *A.* measurement of the core's internal flux status and *B.* balancing or closed-loop control of the flux. Within these two topics, other sub-categorizations are possible, as displayed in Fig. 2 and discussed in the following sections.

A. Flux Measurement / Saturation Detection

The methods for recognition of the core's flux state can be classified into 1) *saturation detection*, 2) *dynamic flux measurement* and 3) *continuous flux behavior measurement*. The measurement method proposed in this paper lays in this last class.

1) **Saturation Detection:** In [2], an E-core was used with an air-gap in one of the external legs (Fig. 3-a)). During normal operation, the flux flows only in the un-gapped leg

but as soon as this leg saturates, a flux is forced to the gapped leg and therefore a voltage can be induced in an additional winding, detecting the saturation of the main flux path. Alternatively, in [3] a slot is placed in one of the core legs, as shown in Fig. 3-b) in order to reduce the cross section area in this place. An additional magnetic path with a winding is provided parallel to the slotted part of the core. As the slotted section has a smaller area, it saturates before the rest of the core and magnetic flux is forced into the parallel magnetic path. This induces a voltage in a winding indicating the impending core saturation.

With both these methods, only the saturation of the core is detected, which may be enough in some applications. In applications which require high efficiency, however, this is not enough since the flux density in the core can still be biased without being saturated and therefore the core losses are increased. Moreover, to implement both these methods, modifications to the magnetic components are required, increasing costs and complexity.

2) **Dynamic Flux Measurement:** This method was proposed in [4] to detect flux unbalance due to variations in the converter loading conditions. The principle is to perform an integration of the applied voltage through an RC network or an active integrator (cf. Fig. 3-c)). This integrated signal is proportional to the core's magnetic flux. Due to the requirement of an integration, this method can only sense dynamic variations of the flux, i.e. steady state asymmetries will not be detected.

3) **Continuous Flux Behavior Measurement:** The sensing of the flux behavior with large bandwidth and independent of the operating conditions has been covered by several publications, where the following main categories can be identified:

a) **Magnetizing Current Measurement:** The magnetizing current $i_m(t)$ indicates the status of flux density in the

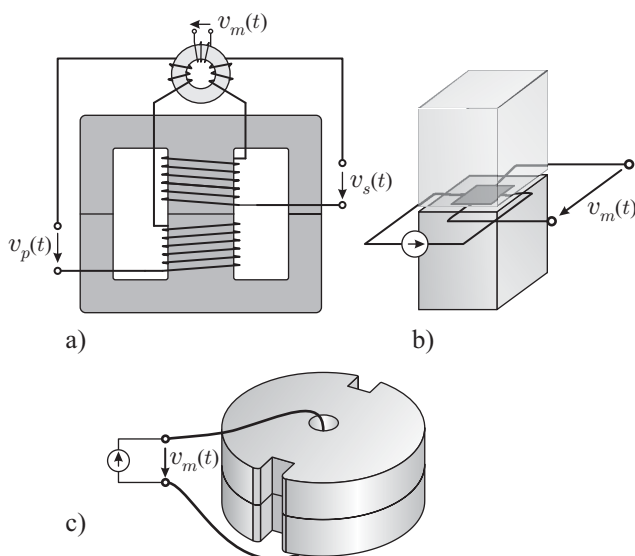


Fig. 4. Continuous measurement of core's internal flux: a) Construction of magnetizing current with external transformer [5], b) Magnetic flux measurement with hall sensor in magnetic path; c) Orthogonal magnetic fluxes [6].

core. The measurement of this current through subtraction of the scaled primary and secondary currents was proposed in [4].

In [5] and later in [7], a measurement of the magnetizing current was performed by building an additional transformer with the same turns ratio as the main transformer but with one of the windings in the inverted orientation (cf. Fig. 4-a). As the primary and secondary currents flow through this transformer, most of the magnetic flux is canceled out and the remaining flux, which is proportional to the magnetizing current, is measured with an additional winding.

The disadvantage of this method is the requirement of isolation on the additional transformer, which needs to be at least the same as the one of the main core. Also, practical issues may arise in higher power transformers where the wiring of primary and secondary sides has an increased complexity.

b) **Orthogonal Magnetic Fluxes:** In [6] the internal core flux was measured by using an additional coil fed by a DC current which generates a magnetic flux orthogonal to the main flux (cf. Fig. 4-c)). The orthogonality of the magnetic fluxes ensures that no voltage is induced in the additional coil due to the main flux. As the main magnetic flux density is changed, the B-H characteristic of the material is also changing. This material property change is translated in a variation of the flux in the orthogonal coil, inducing a voltage in its terminals. This principle was also proposed for microfabricated inductors [8] to intentionally shape the B-H loop of the magnetic material. In this concept, modified or specially shaped cores are required to insert the orthogonal winding, increasing its cost and complexity. Moreover, if the B-H loop has a large linear zone, voltage would be induced in the orthogonal coil only when the core is saturated.

c) **Converter Current Measurement and Processing:** The direct measurement of the primary and/or the secondary currents has also been used to balance the flux in the core. As an example, the DC magnetization of the core generates primary/secondary currents with even numbered Fourier components. The amplitude of these components can be measured and used as feedback signal to balance the transformer flux, as was performed in [9].

In converters with modulations which do not operate always at 50% duty cycle, only the magnetizing current is present during the freewheeling periods. This current can be measured during these intervals obtaining information about the status of the core's flux.

d) **Flux Observer:** To overcome the limitation of only dynamic flux measurement, the method described in **Section II-A2** can be complemented with a measurement of the transformer current [4]. This way, an observer that reconstructs the flux density based on these two signals can be implemented.

e) **Hall Sensing:** The most direct way to measure the flux in the core would be to insert a thin hall sensor in the magnetic flux path [10] (cf. Fig. 4-b)). However, this requires the insertion of an air gap in the magnetic core, reducing the magnetizing inductance and increasing the reactive power provided to the transformer.

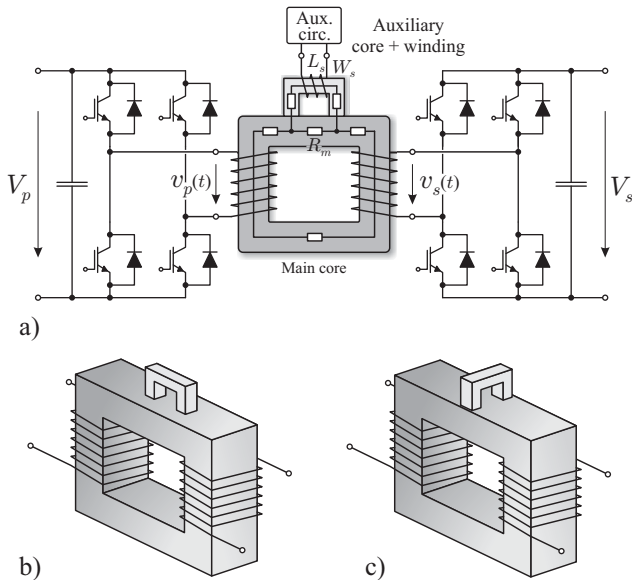


Fig. 5. a) Proposed flux density measurement concept with auxiliary core and winding sharing magnetic path with the main core. The auxiliary core can be placed so that its flux is b) parallel or c) orthogonal to the main flux. The auxiliary core is not shown to scale.

B. Flux Balancing / Feedback Control

The internal core flux can be passively or actively balanced. Depending on whether the measuring principle detects core saturation or performs a complete flux measurement, the active flux balancing principles can be subdivided into saturation correction or continuous flux control.

1) **Passive Balancing:** Passive balancing refers to any balancing principle which does not modify the switching behavior of the semiconductor devices in order to keep the transformer flux between safe margins. The following passive flux balancing principles can be pointed out:

a) **Series Capacitor:** One of the most utilized flux balancing principles, due to its simplicity, is the inclusion of a capacitor in series to the transformer winding. The main disadvantages of this approach are (1) increased converter volume, (2) increased converter losses and (3) slow dynamic response. This idea was further developed in [11] where a resistor was placed in parallel to the capacitor in order to improve low-frequency behavior.

b) **Air-gap in Core's Magnetic Path:** When an air-gap is included in the core's magnetic path, the permeability of the core is effectively decreased. This in turn increases the tolerable DC magnetization but doesn't eliminate the DC flux component as with a series capacitor, thus this is not strictly a flux balancing method. Moreover, the inclusion of an air-gap in the core decreases the value of magnetizing inductance L_m , increasing the switched and conducted currents.

In addition to the previously presented passive flux balancing principles, the prevention of core saturation can be included as part of the converter design process. In [1] the different converter electrical parameters that influence the core saturation were clearly pointed out and used to give design considerations which help avoiding it.

2) **Active Saturation Correction:** The flux measuring concepts presented in Section II-A1 can be used to implement feedback control which only operates under impending core saturation, as was done in [2].

3) **Active Feedback Control of the Flux:** If a signal proportional to the internal core flux density is available, the DC magnetization of the core can be actively controlled by modifying the volts-seconds applied to the transformer. The main feedback flux control principles that have been proposed are detailed in [4–6, 10, 12]. The feedback scheme proposed in this paper is revised in Section IV.

III. PROPOSED FLUX MEASUREMENT METHOD

This section introduces the proposed flux density transducer. First, the working principle is explained and afterwards this principle is experimentally verified using an adequate test circuit.

A. Working Principle

The proposed flux measurement concept is explained through Fig. 5-a). Here, the main core and an auxiliary core with a winding W_s and an inductance L_s are displayed. This additional core is attached to the main core so that they share a part of the magnetic path, represented by the reluctance R_m in Fig. 5-a). The value of the inductance L_s measured at the terminals of the auxiliary winding W_s decreases with increasing value of reluctance R_m . This reluctance in turn is inversely proportional to the relative permeability μ_r of the main core. Therefore, as the core is driven closer to saturation, the value of μ_r is decreased, increasing R_m and finally decreasing the measured inductance L_s . This drop in inductance would thus directly indicate that the main core is entering the saturation region.

This principle was tested in two different cores: a gapped E55 N27 E ferrite core and a AMCC80 Amorphous C-cut core. The auxiliary core is half of a E25 N87 core with an auxiliary winding consisting on 14 turns. It should be noted that the auxiliary core can be placed on the surface of the main core so that their magnetic fluxes are parallel (Fig. 5-b)) or, in order to avoid induced voltages in the auxiliary winding, orthogonal to each other (Fig. 5-c)). The measured inductance for different magnetization levels is shown in Fig. 6-a) and b) for the Ferrite and AMCC80 cores respectively. Additionally, the positive part of the respective B-H loops is displayed. In case of the ferrite core, a clear drop in the measured inductance with both parallel and orthogonal placements can be seen around 0.35 T where the core enters saturation region. In case of the AMCC80 core, as shown in the upper part of Fig. 6-b), its B-H loop is characterized by a continuous decrease of permeability, thus a smooth drop in inductance is measured as the core's magnetic field is increased.

B. The Magnetic Flux Density Transducer: The "Magnetic Ear"

In order to measure the inductance seen from the terminals of W_s (cf. Fig. 5-a)), an auxiliary circuit is required. The utilized circuit in this case is shown in Fig. 7. Here, a half-bridge applies a square-shaped voltage $v_{aux}(t)$ excitation with high-frequency to the auxiliary winding. This frequency

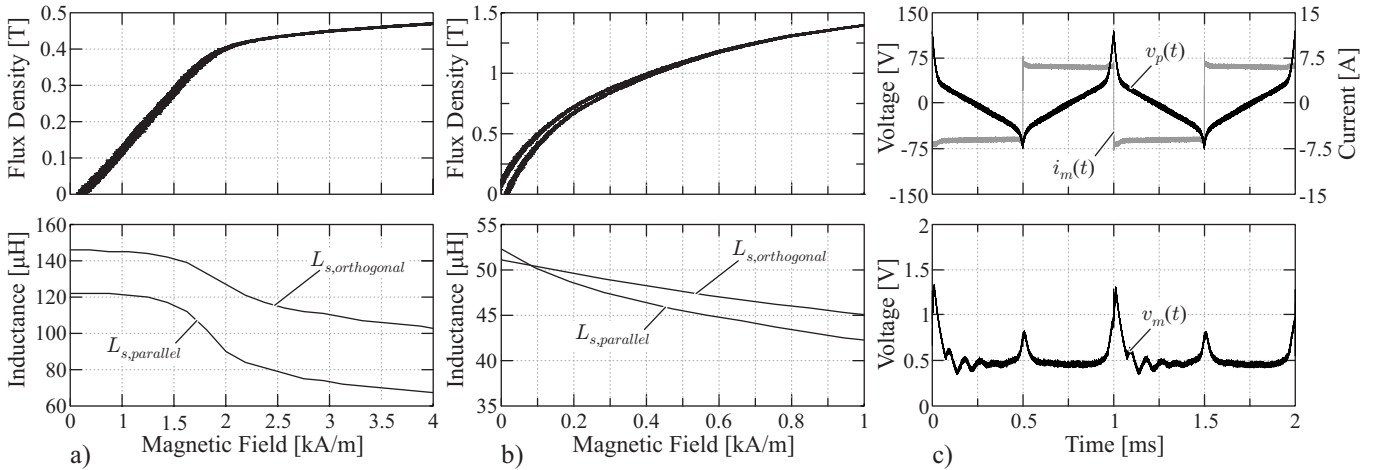


Fig. 6. B-H loops and inductance measurement results on a) ferrite core b) AMCC80 Metglas core. In the upper part of c), a square-shaped voltage applied to the mentioned ferrite core drives the core to saturation. The change in permeability is shown in the lower part of c), which was sensed using the circuit presented in Fig. 7-a).

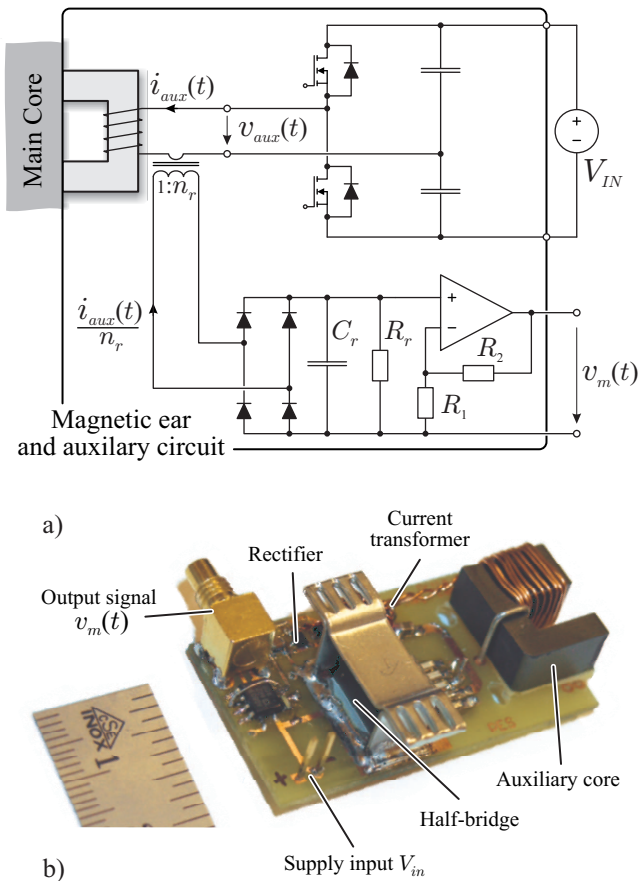


Fig. 7. a) The magnetic ear's driving auxiliary circuit. A half-bridge applies a square-shaped voltage with high frequency to the magnetic ear winding. The current through this core is measured and rectified to obtain a voltage inversely proportional to the inductance of the auxiliary core; b) The Magnetic Ear hardware realization.

needs to be several times higher as the main core excitation. The applied square shaped voltage generates a triangular shaped current $i_{aux}(t)$ through the winding, whose peak

value is inversely proportional to the auxiliary inductance value. This current is sensed with a current transformer and rectified with a full-wave diode rectifier. The rectified current is fed to an RC network for low-pass filtering and finally amplified to obtain signal $v_m(t)$ which is inversely proportional to the auxiliary inductance L_s .

The magnetic flux density transducer, introduced here as the "Magnetic Ear", was tested using the circuit shown in Fig. 8. Here, a single full-bridge converter applies square-shaped voltage with peak value V_p . This way, the magnetizing current $i_m(t)$ can be directly measured and analyzed to study the state of the magnetic flux density in the core. Moreover, an additional winding carrying a DC current I_d is placed around the main core in order to intentionally force a DC flux density component in the core.

The results of the test are shown in Fig. 6-c). Here, a 1 kHz square-shaped voltage is applied to the winding and, as can be noticed from the peaks in the magnetizing current $i_m(t)$, the core is driven into saturation. Additionally, a DC bias in the flux density is observed since the magnetizing current has a non-symmetric shape. The output of the Magnetic Ear is shown in the lower part of Fig. 6-c) where high peaks in the output signal $v_m(t)$ are detected when the core is taken to saturation. It should be noted that the output signal of the

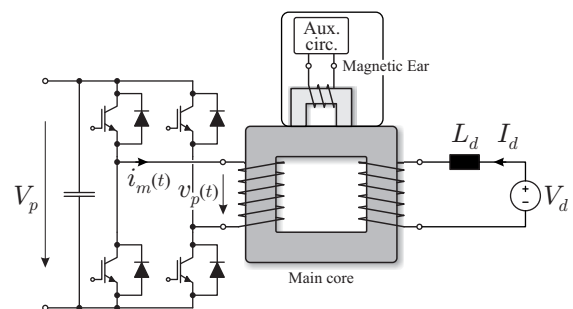


Fig. 8. Test circuit used to analyze the performance of the Magnetic Ear. A single full-bridge converter is used to magnetize the core and an external circuit is used to impose a DC flux density in the core.

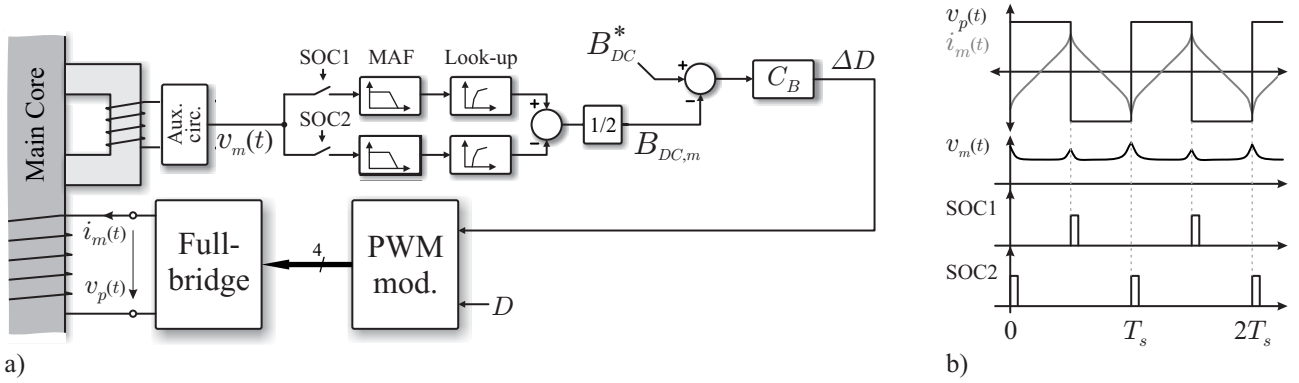


Fig. 9. a) Feedback/balancing scheme: the output of the magnetic ear, $v_m(t)$ is sampled by the ADC in the DSP board. By sampling on each switching event of the full-bridge (part b)), a construction of the DC flux density in the core is obtained and used to balance the flux in the main core.

Magnetic Ear is higher when the full-bridge switches from positive to negative as it is when switching from negative to positive. This shows that the flux density contains a DC component and also gives information about the polarity of this DC bias. The means to use this signal to compensate the DC bias in the core will be now discussed

IV. CLOSED LOOP CONTROL OF THE DC FLUX DENSITY COMPONENT

The output $v_m(t)$ of the Magnetic Ear must be fed into the DSP controller of the full-bridge converter in order to actively compensate the DC-bias. To obtain the value of B_{DC} in the main core, the scheme shown in Fig. 9-a) was used. As can be seen from Fig. 9-b), different Start of Conversion (SOC) signals (the signals that trigger a conversion of the analog-to-digital converter of the DSP), i.e. SOC1 and SOC2 are generated in the positive and negative edges of the full-bridge output voltage $v_p(t)$. The sampled values at each of these instants are independently stored and filtered by Moving Average Filters (MAF). To obtain the final flux density value, a look-up table is built based on the measurements of the Magnetic Ear output and the magnetic flux density calculated from the voltage applied to the core. It should be noted that the gain from the Magnetic Ear output to flux density is highly non-linear since, when the core is close to saturation, a small increase in the flux density generates a large change in the output signal of the transducer whereas, when the core is in linear region, the change in output signal with respect to changes in the flux density is several times smaller.

The output of the look-up tables are the absolute values of flux density in the main core at the switching instants. Therefore, the subtraction of these two signals gives twice the value of DC flux density component B_{DC} inside core. For example, in steady state operation, if no DC bias is present in the core, the output of the Magnetic Ear would be identical at the positive and negative edges of the applied voltage $v_p(t)$. As a consequence, the output of the look-up tables, the flux density at the switching times, would be identical and thus the measured DC flux density component would be zero.

To control the DC flux density in the core, a standard

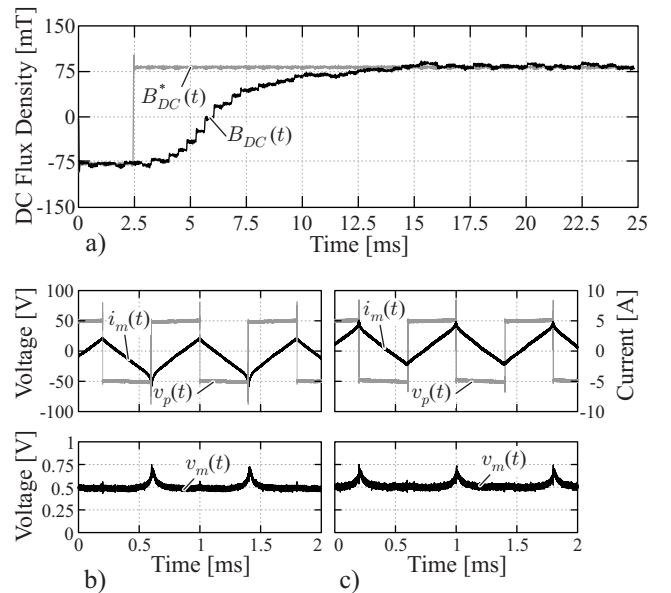


Fig. 10. Closed loop results for step response in the DC flux density reference B_{DC}^* : a) Response of the measured flux density to an increase in reference from -75 mT to 75 mT. The behavior of the applied voltage $v_p(t)$, the magnetizing current $i_m(t)$ and the Magnetic Ear output signal $v_m(t)$ b) before and c) after the step application is also shown.

PI controller, C_B is used (cf. Fig. 9-a)). The output of this controller is the additional duty cycle ΔD required to increase or decrease the DC voltage applied to the primary winding. In the PWM modulator, this signal is combined with the duty cycle D calculated to transfer desired amount of power, which was left to 50% in this case.

Two tests were performed to analyze the performance of the closed loop compensation method: A. step response and B. disturbance compensation. These tests were performed using the ferrite core with a 1.25 kHz square shaped voltage whit peak value of 50 V.

A. Step Response

In Fig. 10-a), the response to a step in the DC flux reference value (keeping the disturbance current I_d of the

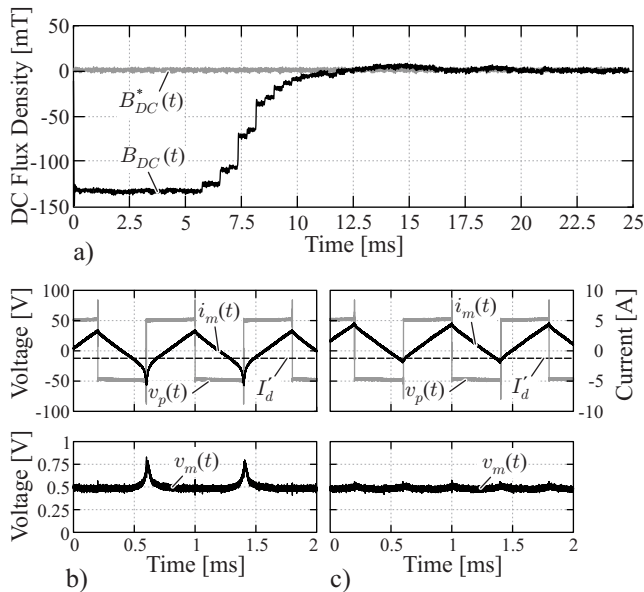


Fig. 11. Closed loop results for disturbance compensation: a) Response of the measured flux density to an externally applied DC flux density of -130 mT; The behavior of the applied voltage $v_p(t)$, the magnetizing current $i_m(t)$ and the Magnetic Ear output signal $v_m(t)$ b) before and c) after the activation of the feedback compensation.

external circuit, cf. Fig. 8, at zero) from -75 mT to 75 mT is displayed. As can be seen, the flux density reference is followed closely by the measurement. The behavior of the magnetizing current $i_m(t)$ and the output of the Magnetic Ear $v_m(t)$ before and after the step application are displayed in Fig. 10-b) and -c) respectively. Before the step application, the magnetizing current $i_m(t)$ features a negative DC bias, which is generating the -75 mT set as reference. After the step application, the DC value of this current has a positive DC bias, meaning that the DC flux density component has changed its polarity. It is worth to note that, before the step application, the output signal $v_m(t)$ of the Magnetic Ear has its peaks in at the positive edges of the applied voltage $v_p(t)$, meaning that at these points the highest flux density value is encountered. After the application of the step, the peaks appear at the negative edges of the applied voltage, i.e. 180° phase-shift with respect to the starting condition, which shows that the DC flux density has changed its polarity.

B. Disturbance Compensation

Using the external circuit shown in Fig. 8, a DC flux density of -130 mT component is imposed in the main core to test the performance of the feedback compensation to external disturbances. To do this test, first the external disturbance is imposed in the core without feedback compensation of the flux density. Later, the compensation is activated.

The results of this test are shown in Fig. 11-a), where the disturbance current I'_d reflected to the primary side (the full-bridge output side) is shown. The compensation is turned on around $t=5$ ms and, as can be seen, the feedback compensation scheme is able to bring the DC flux density component back to zero in spite the externally forced DC flux density. The magnetizing current before the disturbance

application, shown in Fig. 11-b), features no DC component but, however, the output of the Magnetic Ear has clear peaks at the positive edges of the the full-bridge output voltage, meaning that the DC flux density component in the core is negative. After the feedback compensation is activated (cf. Fig. 11-c)), the magnetizing current $i_m(t)$ shows a DC component which compensates for the externally applied DC flux, which is the inverted value of current I'_d . The output signal from the Magnetic Ear has equal peaks at the switching events, which shows that the flux density operates under balanced conditions.

C. Comments on Compensation Scheme Bandwidth

As shown in Figs. 10 and 11, the time constant of the closed loop compensation scheme is around 8 ms, which is equivalent to 10 switching cycles of the full-bridge converter. This time can be reduced by implementing a feed-forward scheme which uses the measured DC flux density B_{DC} signal, since the required volts-seconds required to compensate a given DC bias in the flux density can be easily calculated. Thus, a cycle-per-cycle compensation could be implemented to avoid DC magnetization due to, for example, loading condition variations. Other techniques such as a dead-beat control could be implemented in order to increase the bandwidth of the compensation loop.

Since the switching frequency in medium-frequency applications, where the Magnetic Ear would provide considerable benefits, is relatively low, a sampling frequency several times higher than the main converter's switching frequency could be achieved. This way, a continuous tracking of the flux density would be possible and thus a faster compensation loop would be feasible.

V. CONCLUSIONS

A new magnetic flux density transducer, the Magnetic Ear, has been introduced in this paper. The basic working principle of this transducer is the sharing of magnetic path between the main core and an auxiliary one. The influence of the main flux in this shared magnetic path is sensed by measuring the inductance in an additional winding in the auxiliary core. An auxiliary circuit is used to obtain a signal inversely proportional to the inductance in the auxiliary winding. This signal is fed to a DSP which, based on sampling at the switching events of the driving full-bridge, constructs the signal proportional to the DC flux density component inside the core. With this signal, a closed loop compensation was successfully tested under step changes in the DC component reference and external DC flux disturbances, thus the proposed concept can be implemented in isolated DC-DC converter to avoid DC magnetization of the transformer core.

REFERENCES

- [1] K. O'Meara, "Passive Balancing of Transformer Flux in Power Converters," in *Proc. of the 10th National Solid-State Power Conversion Conference (POWERCON)*, vol. A1, March 1983, pp. 1-11.
- [2] R. Patel, "Detecting Impending Core Saturation in Switched-Mode Power Converters," in *Proc. of the 7th National Solid-State Power Conversion Conference (POWERCON)*, vol. B3, March 1980, pp. 1-11.

- [3] S. Klopper and J. A. Ferreira, "A Sensor for Balancing Flux in Converters with a High-Frequency Transformer Link," *IEEE Transactions on Industry Applications*, vol. 33, pp. 774–779, May/June 1997.
- [4] D. Wilson, "A New Pulsewidth Modulation Method Inherently Maintains Output Transformer Flux Balance," in *Proc. of the 8th National Solid-State Power Conversion Conference (POWERCON)*, vol. D1, April 1981, pp. 1–14.
- [5] F. Stögerer, J. W. Kolar, and U. Drofenik, "A Novel Concept for Transformer Volt Second Balancing of VIENNA Rectifier III Based on Direct Magnetizing Current Measurement," in *Proc. of the Nordic Workshop on Power and Industrial Electronics Workshop*, June 2000, pp. 134–139.
- [6] W. M. Polivka, A. Cocconi, and S. Cuk, "Detection of Magnetic Saturation in Switching Converters," in *Proc. of the PCI Conference*, March 1982, pp. 584–597.
- [7] A. Gerstman and S. Ben-Yaakov, "Zeroing Transformer's DC Current in Resonant Converters with no Series Capacitors," in *Proc. of the Energy Conversion Congress and Exposition*, September 2010, pp. 4028–4034.
- [8] L. Daniel, C. R. Sullivan, and S. R. Sanders, "Design of Microfabricated Inductors," *IEEE Transactions on Power Electronics*, vol. 14, pp. 709–723, July 1999.
- [9] R. Kuttner, "Circuit Techniques for Eliminating Primary Current Unbalance in Push-Pull Power Converters," in *Proc. of the 7th National Solid-State Power Conversion Conference (POWERCON)*, vol. F2, March 1980, pp. 1–9.
- [10] F. P. Dawson, "DC-DC Converter Interphase Transformer Design Considerations: Volt-Seconds Balancing," *IEEE Transactions on Magnetics*, vol. 26, pp. 2250–2252, September 1990.
- [11] R. Redl, N. Sokal, and C. W. Schaefer, "Transformer Saturation and Unusual System Oscillations in Capacitively Coupled Half-Bridge or Full-Bridge Forward Converters: Causes, Analyses, and Cures," in *Proc. of the Power Electronic Specialists Conference (PESC)*, April 1988, pp. 820–828.
- [12] S. Han, I. Munuswamy, and D. Divan, "Preventing Transformer Saturation in Bi-Directional Dual Active Bridge Buck-Boost DC-DC Converters," in *Proc. of the Energy Conversion Congress and Exposition*, September 2010, pp. 1450–1451.